

Determining the Forces on the Screws in Two- and Three-Bearing Two-Screw Pumps

V. M. Ryazantsev and V. V. Plyasov

OAO LIVGIDROMASH, Livny

e-mail: ryazancev@livgidromash.ru, plyasov@livgidromash.ru

Abstract—Various methods of determining the forces on screws with different numbers of turns are considered. Formulas are derived for two- and three-bearing screw pumps.

DOI: 10.3103/S1068798X10090066

In creating high-pressure two-screw pumps, we need to know: (1) the hydraulic radial forces on the screws and their direction; (2) the bearing configuration of the pump rotors (screws)—two- or three-bearing pumps; (3) the bearing reactions and their direction, the flexure curve, or the maximum flexure at the danger points.

In the calculation of multiscrew pumps, we need to know the radial and axial forces on the screws due to the pumping of the liquid.

As a rule, two-screw pumps are double-flow pumps, since in that case the axial forces cancel out. Therefore, in the calculation of double-flow two-screw pumps, the axial forces are unimportant, in contrast to the radial forces. In fact, two-screw pumps are characterized by intense unidirectional wear of the ring on account of the low rigidity of the relatively long screws and the considerably larger radial forces.

Various methods of determining the radial forces on the screws of multiscrew pumps were outlined in [1–7]. The most general formulas for the radial forces P_{r1} in single-flow multiscrew pumps were derived in [1]

$$P_{r1} = \left(zpr_e a + 2pr_e a \sin^2 \frac{\xi}{2} \right) + zpr_i b + \frac{z}{2} p(r_i + r_e \cos \xi) \left(\frac{t}{z} - a - b \right), \quad (1)$$

where z is the number of turns of the screw; p is the pressure in the pump; r_e and r_i are the external and internal screw radii; a, b are the widths of the screw projection and depression, respectively, in the axial cross section; ξ is the angle between the center line and the radius of the point of intersection of the external circles; t is the screw pitch [1].

The directions of action of the radial forces are shown in Fig. 1. Looking from the high-pressure side of the pump, we determine the direction of the radial

force by turning center-line segment O_1O_2 by 90° in the direction of screw rotation.

To determine the radial forces on screws of different type, the method in [1] was used in somewhat simplified form in [2]. The most detailed method of determining the radial and axial forces was outlined in [4]; this method was also used in deriving the formulas for two-screw pumps. The ratio D_e/D_i of the screw's external and internal diameters—that is, the relative cutting depth—should be $D_e/D_i = 1.36, 1.4, 5/3$, and 2, according to the recommendations in State Standard GOST 20572–88. Table 1 presents the calculated radial forces P_{r1} for screws with such D_e/D_i values, when the forces act on half of a double-flow screw, as well as the radial forces $P_{r2} = 2P_{r1}$ acting on the whole of the double-flow screw.

We now compare the radial forces obtained by the methods in [1, 4]. For $D_e/D_i = 1.36$, according to Eq. (1)

$$P_{r1} = 0.226213pt(D_e + D_i) + 0.0475574pt(0.5D_i + 0.4338235D_e) = 0.5Atp.$$

Thus $P_{r2} = 2P_{r1} = Atp$.

By contrast, the following radial force is obtained by the method in [4]

$$P_{r2} = 1.113664Atp. \quad (2)$$

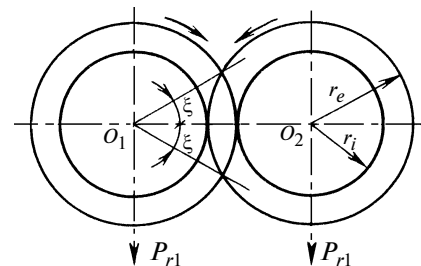


Fig. 1. Direction of radial forces in end cross section of screws.

Table 1

| D_e/D_i | $P_{r1}/(Atp)$ | $P_{r2}/(Atp)$ |
|-----------|----------------|----------------|
| 1.36 | 0.556832 | 1.113664 |
| 1.4 | 0.560124 | 1.120248 |
| 5/3 | 0.576326 | 1.152658 |
| 2 | 0.583535 | 1.167069 |

Table 2

| Screw | Radial forces on double-flow screws | | |
|--------------|-------------------------------------|------------------------|------------------------|
| | single-turn profile $a-b$ | cycloid engagement 1–2 | cycloid engagement 2–3 |
| Drive screw | 1.120248Atp | 1.034703Atp | 1.039586Atp |
| Driven screw | 1.120248Atp | 2.079171Atp | 0.964920Atp |

The discrepancy is less than 10% [1, 4]. Two-screw pumps not only employ single-turn screws (Fig. 2) but also screws with cycloid engagement of types 1–2 (single-turn drive screw and two-turn driven screw, with a cycloid tooth profile) and 2–3 (two-turn drive screw and three-turn driven screw with a cycloid tooth profile). To establish the influence of the number of screw turns, the radial forces are calculated by the method in [4]; we assume that $D_e/D_i = 1.4$ (Table 2).

All the screws, except driven screws with 1–2 cycloid engagement, experience approximately the same load. For 1–2 cycloid engagement, the load on the driven screw is about twice as large. Calculation of the axial forces poses no difficulties [1–4]. Experiments are conducted to verify the formulas obtained. The dependence of the screw flexure on the load G is determined. In pumping liquid through clogged screws, the

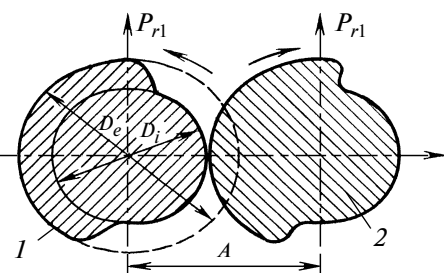


Fig. 2. End cross-section of single-turn screw with asymmetric profile: (1) drive screw; (2) driven screw.

dependence of the screw flexure on the pressure difference p at the pump input and output is also determined. We assume that the pressure distribution over the length of the screws matches that in industrial practice. Hence, the forces on the pump turns are the same. From the dependences $y = f(G)$ and $y = f(p)$, we obtain the formula $G = f(p)$. Comparison with the theoretical formula $P_{r2} = f(p)$ (Table 1) permits refinement of the constant and thus we obtain a useful empirical formula.

For the experiment, we select the mass-produced 2VV 6.3/16 pump. We consider the single-turn screws most commonly used in mass-produced pumps, for which $D_e = 60$ mm, $D_i = 44$ mm, and $t = 14, 18$, and 26 mm. The loading configuration employed in determining $y = f(G)$ is shown in Fig. 3. Turn 2 and its supporting bearings are mounted on supporting prisms 3. Suspension arms 4 (with loads 5) are located at a distance equal to half the screw pitch ($t/2$) from the ends of the segment. The shaft flexure is measured by indicator 1.

In Fig. 4, we illustrate the determination of the screw flexure y as a function of the pressure p in the pump. In screw housing 2, a hole is bored to accommodate a pipe with needle 3. The hole is drilled so that the needle is in the plane passing through the screw axis and perpendicular to the plane passing through the axis of the drive screw and driven screw, while the contact point of the needle and shaft 1 divides the distance between the screw segments in half. The motion of the needle is measured by indicator 4. The pump screws are locked, and oil from another pump is supplied through pressure tube 7. The oil is drawn off to a measuring tank through suction tube 5. The pressure difference is monitored by manometers 8 and 6.

In Fig. 5, we plot the experimental curve $G = f(p)$ and the theoretical curve $P_{r2} = f(p)$ from Eq. (2) for the drive screw 1 and the driven screw 2, with $t = 18$ mm. Such curves are also plotted for other screws. The difference between the theoretical and experimental results is least for the drive screw. To derive the empirical formula, we use the dependence $G = f(p)$ for the driven screw, for which the radial force is greater than for the drive screw. For three screws ($t = 14, 18$, and 26 mm), the mean is $C = P_{r2}/(Atp) = 1.4$. Thus, the recommended formula for single-turn screws with $D_e/D_i = 1.36$ is

$$P_{r2} = 1.4Atp. \quad (3)$$

Analysis of Eqs. (2) and (3) shows that the experimental C value is 25% greater than the theoretical value. Therefore, for other cases, we increase the theoretical load by 25% to obtain the experimental load.

In Fig. 6, experimental curve 1 (dashed curve) takes the form $P_{r2}/(Atp) = f(D_e/D_i)$. It passes through the point with coordinates $D_e/D_i = 1.36$ and $P_{r2}/(Atp) = 1.4$.

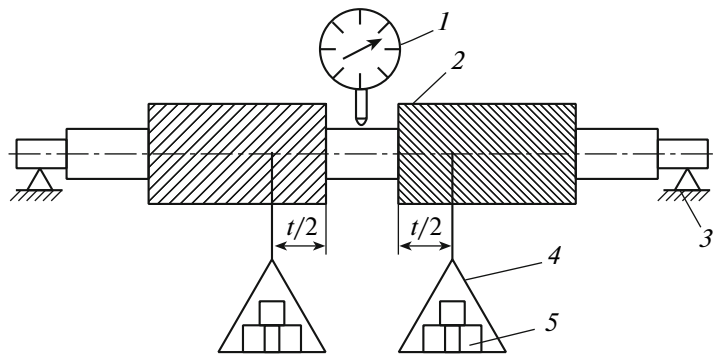


Fig. 3. Screw loading.

and is parallel to theoretical curve 2 (Table 1), which is described by the formula

$$P_{r2} = \left(1.01 + 0.08 \frac{D_e}{D_i} \right) Atp. \quad (4)$$

The empirical formula takes the form

$$P_{r2} = \left(1.29 + 0.08 \frac{D_e}{D_i} \right) Atp. \quad (5)$$

The inverse ratio $v = D_i/D_e$ (the relative magnitude of the hub) was used in [5]. It was shown that the direction and magnitude of the radial force vary in different positions of the rotating screw. A formula for the mean radial force was also derived. Tables 3 and 4 present these parameters when $D_e/D_i = 1.4$ and 2.

The force $P_{r1} = P_{r2}/2$ acts on a single barrel of the screw at a distance $t/2$ from the ends of the drum (Fig. 3). It follows from Eq. (4) that theoretically

$$P_{r1} = P_{r2}/2 = (0.505 + 0.04 D_e/D_i) Atp. \quad (6)$$

From Eq. (5), we obtain the empirical formula

$$P_{r1} = (0.645 + 0.04 D_e/D_i) Atp. \quad (7)$$

For two-screw pumps, it is customary to use single-turn drive screws and driven screws, with 1–1 cycloid engagement and double-turn drive screws and driven screws with 2–2 cycloid engagement. The radial force depends on the length of the closed chamber, which, in turn, depends on the profile employed [5, 11]. In Russia, 1–1 and 2–2 cycloid engagements with the following profiles are employed for two-screw pumps: (1) d (UE); (2) a (UE + OE); (3) b (OG + OE); (4) $b1$ (UE + OG + OE); (5) UE + EV + UKE; (6) OG + EV + OE; (7) UE + OG + EV + OE; (8) UE + OG + EV + UKE + OE; (9) sealed 1–1 cycloid engagements with profile OE + UE and UE ($a-d$) and with profile UE + EV + UKE and UE. (The notation is explained in [11].) The closed-chamber lengths are determined for each profile in [11].

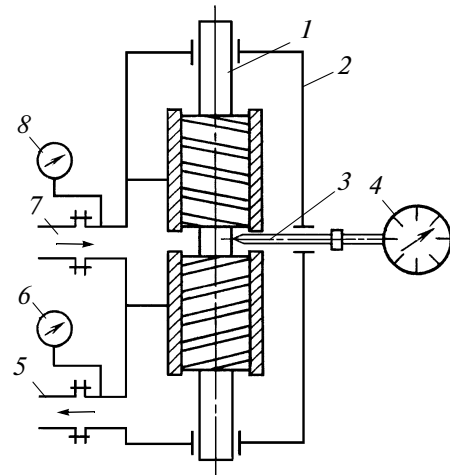


Fig. 4. Determining the screw flexure.

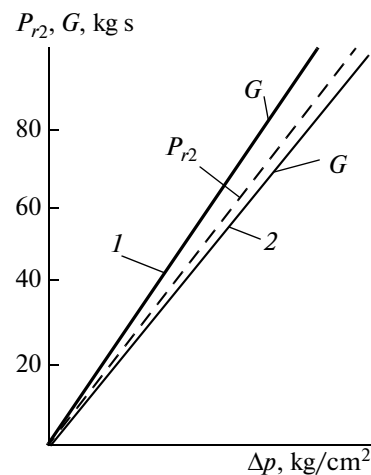


Fig. 5. Dependence of the load G and radial force P_{r2} on the pressure p in single-turn screws: (1) drive screw; (2) driven screw.

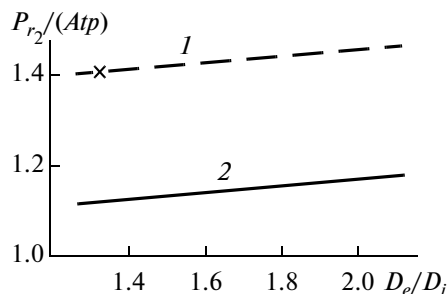
Fig. 6. Dependence of force P_{r2} on D_e/D_i .

Table 3 presents the relative radial force $P_{rl}/(Atp)$ on a single-flow screw (or on a single barrel of a double-flow screw), when $D_e/D_i = 1.4$ for 1–1 cycloid engagements and 2–2 cycloid engagements with profiles *a* and with profiles *a*–*d*; Table 4 presents the corresponding results when $D_e/D_i = 2$. Values are also given for the minimum relative length of the screws, equal to the relative closed-chamber length L_1/t . The calculation is based on different methods [1, 5].

Analysis of Tables 3 and 4 shows that the radial forces given by Eq. (6) are practically the same as the maximum radial forces obtained by the method in [5].

Table 3

| Source, formula | Cycloid engagement 1–1 | | Cycloid engagement 2–2 | |
|-------------------------------------|------------------------|---------|------------------------|---------|
| | $P_{rl}/(Atp)$ | L_1/t | $P_{rl}/(Atp)$ | L_1/t |
| [1] (profile <i>a</i>) | 0.538 | 1.480 | 0.516 | 1.230 |
| [5] (profile <i>a</i>)* | 0.550/0.475 | | 0.538/0.494 | |
| Eq. (6) | 0.561 | | ND** | ND |
| Eq. (7) | 0.701 | | ND | ND |
| [5] (profile <i>a</i> – <i>d</i>)* | 0.540/0.504 | 2 | ND | ND |

Notes: * Maximum/effective (mean) radial force on the screw.

** ND, no data.

See References.

Table 4

| Source, formula | Cycloid engagement 1–1 | | Cycloid engagement 2–2 | |
|-------------------------------------|------------------------|---------|------------------------|---------|
| | $P_{rl}/(Atp)$ | L_1/t | $P_{rl}/(Atp)$ | L_1/t |
| [5] (profile <i>a</i>)* | 0.566/0.488 | 1.445 | 0.537/0.52 | 1.195 |
| Eq. (6) | 0.585 | | ND | ND |
| Eq. (7) | 0.725 | | ND | ND |
| [5] (profile <i>a</i> – <i>d</i>)* | 0.572/0.513 | 2 | ND | ND |

* Maximum/effective (mean) radial force on the screw.

The radial forces for single-turn screws and two-turn screws are also practically the same; the effective (mean) radial force for the two-turn screw is 4–6.6% larger than the force for the single-turn screw. However, the maximum radial force on the single-turn screw is 2.2–5.4% greater than that on the two-turn screw (Tables 3 and 4). The radial forces calculated from Eq. (7), which is obtained experimentally, are considerably greater than the forces obtained theoretically. This difference may perhaps be explained in that the actual torque is greater than the theoretical torque on account of the friction between the working components and the liquid being pumped and correspondingly the actual forces are larger than the theoretical forces. The frictional area is greater for two-turn screws. Therefore, in pumping high-viscosity liquids, the actual force is greater on two-turn screws than on single-turn screws, and this difference will be greater than we see in Tables 3 and 4.

Since the difference in the radial forces on single-turn screws and two-turn screws is considerably less than the difference between the experimental and theoretical radial forces on a single-turn screw, calculations for 1–1 cycloid engagement and 2–2 cycloid engagement may be based on the same formula—Eq. (7), which is obtained experimentally for 1–1 cycloid engagement.

Analysis of Tables 3 and 4 shows that the radial forces on screws with hermetic 1–1 cycloid engagement with profile *a*–*d* are slightly greater than those on screws with profile *a*. Therefore, in improving the manufacture of screws with closed profiles for multiphase pumps, we should use profile *a*–*d*, since the presence of gas in the mixture requires a high degree of sealing of the working components.

In Fig. 7, we illustrate the calculation of a two-screw pump with bilateral input. In Fig. 7, S_1 is the gap between the lateral screw profiles; S_2 is the gap between the tooth tip of one screw and the bottom of the depression for the other screw; S_0 is the gap between the screws and the ring. In this case, the load is greatest on the drive screw. At points A_1 and F_1 , torques are applied, respectively, from the drive (M_{to}) and from the synchronizing gear ($M_{to}/2$); at points C_1 and D_1 , torques are applied from the pumped liquid ($M_{to}/4$). The direction of radial force P_{rl} on the barrel is found by turning segment C_1C_2 through 90° in the direction of screw rotation, when we are looking from the high-pressure section [1]. The determination of the required pump power N_r with specified parameters is outlined in [11]. The torque on the drive screw is $M_{to} = N_r/\omega$, where ω is the speed of the drive screw; the azimuthal forces on the synchronizing gear are $P_0 = M_{to}/A$, where A is the distance between the rotor axes. Table 5 presents the basic screw dimensions, the

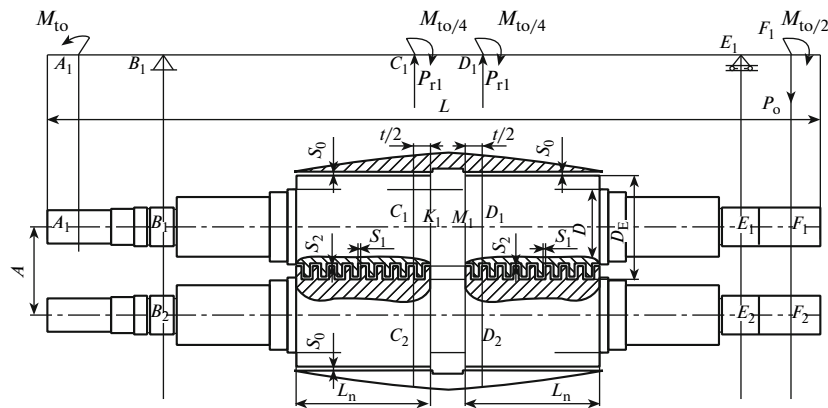


Fig. 7. Calculation scheme for two-screw pump with bilateral input.

unilateral gaps S_0 between the screws and the ring, the relative gap S_0/D_e , and the gaps S_1 and S_2 .

A computer is used for strength and rigidity calculations of stepped shafts. The algorithm for calculating the flexure of multibearing stepped shafts is based on the initial-parameter method. In this method, sections of the screw thread are replaced by a continuous shaft whose diameter is the mean thread diameter $D = (D_e + D_i)/2$. German two-screw pumps include working components with $S_0/D_e = 0.25 \times 10^{-3}$, 0.5×10^{-3} , 1×10^{-3} , and 2×10^{-3} [5]. Most often, $S_0/D_e = 0.5 \times 10^{-3}$ [5]. Approximately the same value ($S_0/D_e = 0.425 \times 10^{-3}$) is used in the A5 2VV 160/25 pump, characterized by the best bulk efficiency.

The flexure of the drive screw is greatest between the two barrels at point K_1 or at the end of the screw at point N_1 (Fig. 7); the flexure at the barrels is greatest at point M_1 . For normal pump operation, the flexure at point M_1 must be less than the gap S_0 between the drum and the ring. In screw flexure, S_1 and S_2 are not as important as S_0 but must rule out mutual contact of the screws. In the absence of contact between the working components, when liquid with any lubricant properties is pumped between them, we observe liquid

friction, characterized by a direct dependence of N_r on the differential pressure p . In the case of nonlubricant liquid—say, water—when the screw flexure is equal to S_0 , the dependence $N_r = f(p)$ is nonlinear; in other words, semiliquid friction appears.

Table 6 presents test data for pumps with water supply. For A5 2VV 160/25 and A3 2VV 63/25 pumps, nonlinearity of the $N_r = f(p)$ curve is observed; for A5 2VV 50/25 and A5 2VV 63/25 pumps, there is no nonlinearity on account of the small screw flexure at rated pressure.

Table 6 shows that the calculated flexure is equal to the gap for the A5 2VV 160/25 pump; this corresponds to nonlinearity of the $N_r = f(p)$ curve. For the A3 2VV 63/25 pump, semiliquid friction sets in at a flexure $W_{m1} = 0.129$, which is less than $S_0 = 0.17$ mm. This may be attributed to manufacturing errors of the working components and poor pump assembly. For the A5 2VV 63/25 and A5 2VV 50/25 pumps, the calculated flexure (0.028 mm) is considerably less than $S_0 = 0.17$ mm. Therefore, liquid friction between the working components may be assumed. This confirms the validity of the formulas for the radial forces on the screws and the calculation scheme.

Table 5

| Pump | Cycloid engagement | Profile | D_e | D_i | t | L_b | L | S_0 | S_1 | S_2 | $S_0/D_e \times 10^3$ |
|---------------|--------------------|-------------------------|-------|-------|-----|-------|------|-------|-------|-------|-----------------------|
| | | | mm | | | | | | | | |
| A3 2VV 63/25 | 2–2 | UE + EV + UKE | 175 | 125 | 56 | 230 | 1320 | 0.17 | 0.15 | 0.3 | 0.971 |
| A5 2VV 50/25 | 1–1 | UE + OG + EV + UKE + OE | 175 | 125 | 36 | 185 | 1016 | 0.17 | 0.1 | 0.1 | 0.971 |
| A5 2VV 63/25 | 1–1 | UE + EV + UKE | 200 | 100 | 30 | 120 | 890 | 0.17 | 0.1 | 0.15 | 0.85 |
| A5 2VV 160/25 | 2–2 | UE + EV + UKE | 200 | 100 | 62 | 210 | 1080 | 0.085 | 0.1 | 0.1 | 0.425 |

Table 6

| Pump | p , MPa | S_0 , mm | P_{rl} , N | W_{m1} , mm |
|--------------|-----------|------------|--------------|---------------|
| A5 2VV160/25 | 1.7 | 0.085 | 11460 | 0.081 |
| A3 2VV 63/25 | 1.8 | 0.17 | 10600 | 0.129 |
| A5 2VV 63/25 | 2.5 | | 8160 | 0.028 |
| A5 2VV 50/25 | 2 | | 7570 | 0.028 |

Table 7

| Pump | p , MPa | S_0 , mm | P_{rl} , N | W_{m1} , mm |
|--------------|-----------|------------|--------------|---------------|
| A5 2VV160/25 | 2.5 | 0.085 | 16860 | 0.119 |
| A3 2VV 63/25 | 2.5 | 0.17 | 14720 | 0.180 |
| | 3 | | 17660 | 0.216 |
| A5 2VV 63/25 | 3 | 0.17 | 9790 | 0.034 |
| A5 2VV 50/25 | | | 11350 | 0.043 |

Oil is characterized by considerable lubricant properties. Therefore, reliable pump operation is possible even when the calculated flexure exceeds S_0 .

Table 7 presents results for pump operation with oil of viscosity $\nu = 0.74 \times 10^{-4} \text{ m}^2/\text{s}$, with a linear $N_r = f(p)$ curve—in other words, with liquid friction between the working components.

For A5 2VV 160/25 and A3 2VV 63/25 pumps, $W_{m1} > S_0$, but the $N_r = f(p)$ curve is linear. For A5 2VV 63/25 and A5 2VV 50/25 pumps, $W_{m1} < S_0$.

A three-bearing system is used in the A8 2VV 50/40-30/40, A8 2VV 80/40-40/40, A8 2VV 125/40-80/40, and A8 2VV 8/50-4/30 pumps at $p = 4 \text{ MPa}$ [7–10].

The A5 2VV 50/25-40/20 (A5 50/25) multiphase pump is designed for water supply at $p = 2 \text{ MPa}$. The A8 2VV 50/40-30/40 (A8 50/40) pump has the same geometry of the working components as for the A5 50/25 two-bearing pump, but includes an extra bearing for the synchronizing gears. This reduces shaft flexure at the synchronizing gears, the barrels, and the clutch.

In Fig. 8, we show the flexure of the drive screw in the A8 50/40 two-bearing pump when $p = 4 \text{ MPa}$; in Fig. 9, we show the corresponding graph for a three-bearing pump. At $p = 4 \text{ MPa}$, the radial hydraulic force on a single barrel at a distance $t/2$ from the high-pressure end is found from Eq. (7): $P_{rl} = 15140 \text{ N}$. Since the profiles of the drive screws and driven screws are the same, the hydraulic torques on the screws will also be the same. Hence, the radial force on the synchronizing gear is $P_3 = M/A = 6270 \text{ N}$, where $M = N/\omega = 941 \text{ N m}$ is the torque at the pump shaft; $N = 140 \text{ kW}$ is the pump power required when $\nu = 10^{-3} \text{ m}^2/\text{s}$; $\omega = 151.84 \text{ rad/s}$ is the drive speed; $A = 0.15 \text{ m}$.

In a three-bearing pump, the screw flexure is less than in a two-bearing pump (Figs. 8 and 9):

the maximum flexure at the synchronizing gears is

$$y_{N_2}/y_{E_3} = -0.085/(-0.0075) = 11.3;$$

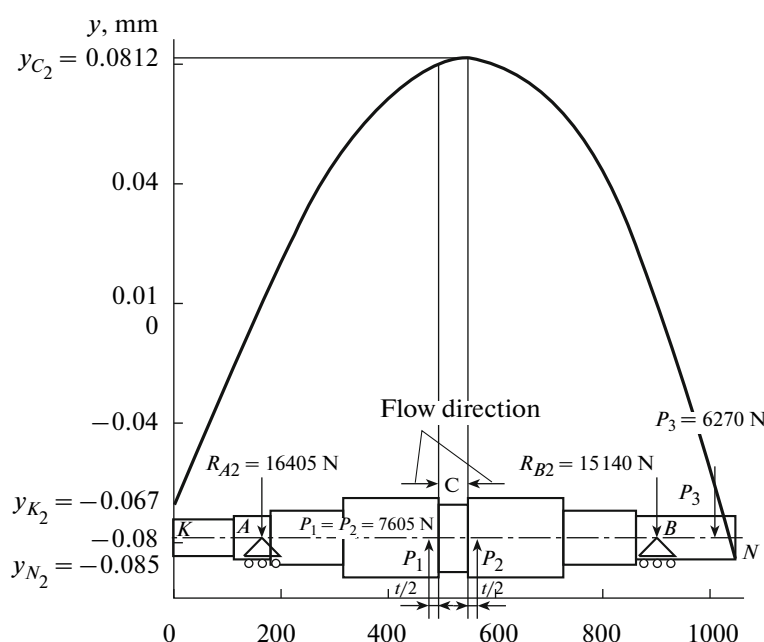


Fig. 8. Drive-screw flexure in A8 2VV 50/40-30/40 two-screw pump at $p = 4 \text{ MPa}$.

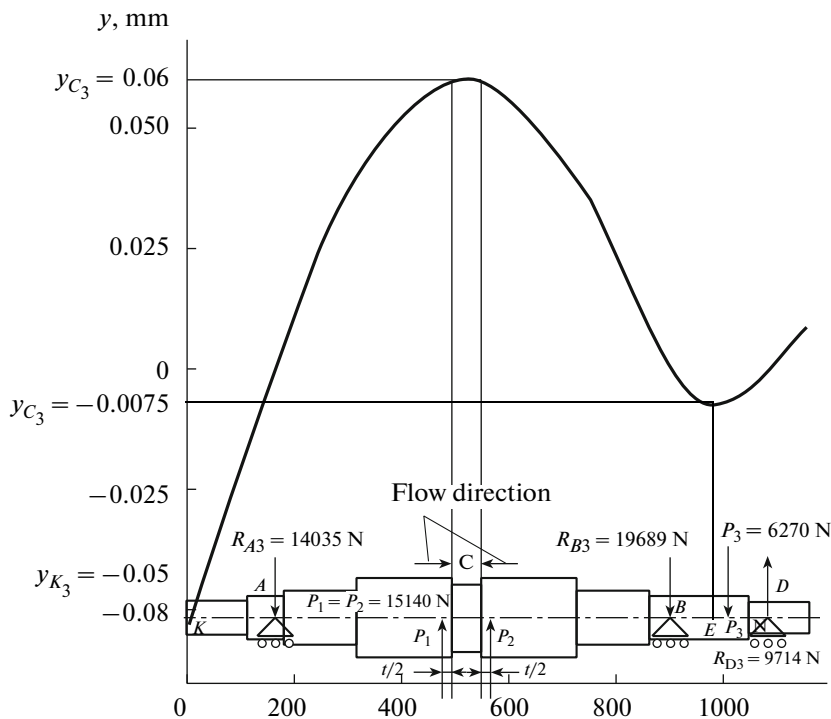


Fig. 9. Drive-screw flexure in A8 2VV 50/40-30/40 three-screw pump at $p = 4$ MPa.

the flexure around the barrel ring (at point *C*) is

$$y_{C_2}/y_{C_3} = 0.0812/0.06 = 1.35;$$

the maximum flexure at the clutch is

$$y_{K_2}/y_{K_3} = -0.067/(-0.05) = 1.34.$$

A deficiency of the three-bearing structure is increased radial force on bearing *B*: $R_{B_3}/R_{B_2} = 19689/7605 = 2.59$.

The force on bearing *A*, conversely, is somewhat reduced: $R_{A_3}/R_{A_2} = 14035/16405 = 0.855$.

A benefit of the three-bearing structure is improved operation of the synchronizing gears.

To eliminate screw contact with the ring while maintaining acceptable bulk efficiency, we specify the following dimensions of the working components and tolerances: $D_e = 175^{-0.3}_{-0.35}$ H7; $D_i = 125^{+0.08}_{+0.07}$; diameter of aperture in ring $175^{+0.05}_{+0.02}$; $A = 150^{+0.02}$; the pitch of the single-turn screw $t = S = 36$; barrel length $L = 180$; $S_0 = 0.16-0.175$; $S_1 = 0.1-0.125$; $S_2 = 0.135-0.14$; $S_0/D_e = (0.914-1) \times 10^{-3}$; $S_1/D_e = (0.571-0.714) \times 10^{-3}$; $S_2/D_e = (0.771-0.8) \times 10^{-3}$.

The three-bearing structure permits doubling of the pressure! The screw profile UE + OG + EV + UKE + EV facilitates reliable pump operation and

increased working life of the cutting tool in screw production [11].

Note that the small screw pitch ($t = 36$, $t/D_e \approx 0.206$) reduces the radial force on the screw, which is directly proportional to the pitch, as we see in Eqs. (2) and (3), and increases the number of closed chambers over the length of the drum: $N = L/S - 0.5 = 4.5$. In addition, dynamic balancing is simpler with smaller pitch of the single-turn screw.

The A8 2VV 125/40-80/40 (2VV 125/40) pump differs from the A8 2VV 80/40-40/40 (2VV 80/40) pump only in the pitch of the single-turn screw ($t = 46$ mm, rather than $t = 30$ mm) [8]. In addition, a smoother lateral profile is employed: UE + OG + EV + UKE + OE, rather than UE + EV + UKE [11]. This reduces the wear when the pumped liquid contains abrasive and extends the tool life in cutting the screws [11].

The three-bearing 2VV 125/40 pump is made in two versions: with a rear gear (Fig. 10) in the housing of the 2VV 80/40 pump [8]; and with a front gear (Fig. 11), with improved cooling of the synchronizing gears by an air flux from the electric motor. The additional bearing practically eliminates flexure of the shaft in the region of the gears, which reduces mechanical losses and noise. In addition, screw flexure is reduced, which is important for two-bearing pumps, since screw contact with the ring is impermissible.

In Fig. 10, we illustrate the calculation of the flexure of drive screws and driven screws in the vertical

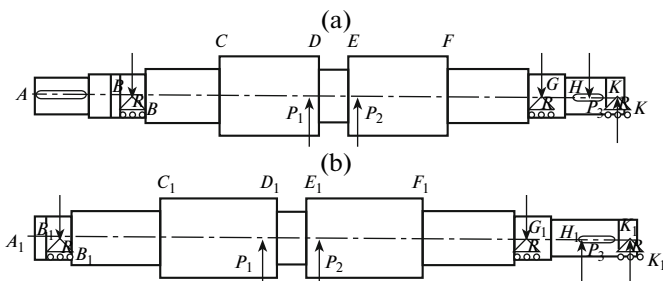


Fig. 10. Calculation of flexure and bearing reaction for drive screw (a) and driven screw (b) of 2VV 125/40 pump with rear gear.

plane and the bearing reactions for 2VV 125/40 pumps with a rear gear; in Fig. 11, we illustrate the same calculation for a pump with a front gear.

To rule out screw contact with the ring, while retaining bulk efficiency, we specify the following dimensions of the working components and tolerances: $D_e = 200_{-0.40}^{+0.35}$; $D_i = 100_{-0.10}^{+0.15}$; diameter of aperture in ring 200 H7; $A = 150_{-0.03}^{+0.03}$; $t = S = 46$; $L = 230$; $S_1 = 0.12-0.15$. For pumps with a front gear, $S_0 = 0.16-0.18$; $S_1 = 0.18-0.22$; $S_2 = 0.18-0.22$ (according to the drawing, $S_2 = 0.1-0.15$); $S_0/D_e = (0.8-0.9) \times 10^{-3}$; $S_1/D_e = S_2/D_e = (0.9-1.1) \times 10^{-3}$.

The pump is intended to supply water at $p = p_{\text{out}} - p_{\text{in}} = 4$ MPa. Tests with the supply of water and water-air mixture are conducted using a booster centrifugal pump, which ensures an input pressure $p_{\text{in}} = 0.3-0.4$ MPa at the two-screw pump. The geometric supply of the pump with a shaft speed $n = 1450$ rpm is 167.54 m³/h. The 2VV 125/40 three-bearing pump ensures operation at $p = 4$ MPa for oil or water supply and also with brief

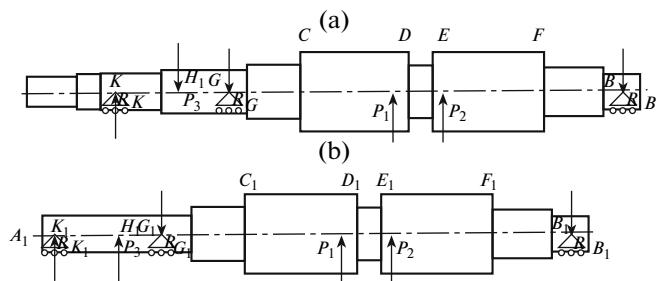


Fig. 11. Calculation of flexure and bearing reaction for drive screw (a) and driven screw (b) of 2VV 125/40 pump with front gear.

pumping of gas locks. The pump power required for designs with front and rear gears is practically the same. To compare the designs by the initial-parameter method, we determine the flexure at the most important points of the screws and the bearing reactions (Figs. 10 and 11).

Besides the three-bearing structure, a two-bearing pump with a rear gear is considered, without an additional bearing for the synchronizing gear. In tests of the 2VV 125/40 pump with a rear gear at $n = 1450$ rpm, $p = 4$ MPa, and $v = 70$ mm²/s, we determine the torques at the synchronizing gear $M_{\text{to}} = -1254$ N m, at the barrels $M_1 = M_2 = 313.5$ N m, and at the synchronizing gear $M_3 = 627$ N m; the radial force at the gear $P_3 = -8360$ N; and the radial forces at the barrels $P_1 = P_2 = 20010$ N (Fig. 10).

Table 8 presents the flexure of the drive screw at the most important points for these three pumps. Although the maximum screw flexure structure is between points D and E, the flexure at points D and E determines the minimum permissible gap between the

Table 8

| Point | Gear position | | | | | |
|-------|---------------------------|--------|--------------|--------|---------------------------|--------|
| | rear | | | | front | |
| | three bearings (Fig. 10a) | | two bearings | | three bearings (Fig. 11a) | |
| | y, mm | R, N | y, mm | R, N | y, mm | R, N |
| A | -0.0809 | - | -0.1022 | - | 0.0364 | - |
| B | 0 | -17555 | 0 | -20660 | 0 | -18260 |
| C | 0.0824 | - | 0.1054 | - | 0.0636 | - |
| D | 0.1364 | - | 0.1807 | - | 0.1293 | - |
| E | 0.1347 | - | 0.1809 | - | 0.1304 | - |
| F | 0.0646 | - | 0.1046 | - | 0.0723 | - |
| G | 0 | -28993 | 0 | -11000 | 0 | -24679 |
| H | -0.0109 | - | -0.0809 | - | -0.0145 | - |
| K | 0 | 14888 | - | - | 0 | 11279 |

Table 9

| Point | Gear position | | | | | |
|-----------------------|---------------------------|--------------|---------------|--------------|---------------------------|--------------|
| | rear | | | | front | |
| | three bearings (Fig. 10b) | | two bearings | | three bearings (Fig. 11b) | |
| | <i>y</i> , mm | <i>R</i> , N | <i>y</i> , mm | <i>R</i> , N | <i>y</i> , mm | <i>R</i> , N |
| <i>A</i> ₁ | -0.00807 | - | -0.0098 | - | 0.005 | - |
| <i>B</i> ₁ | 0 | -18050 | 0 | -19514 | 0 | -18024 |
| <i>C</i> ₁ | 0.0623 | - | 0.0708 | - | 0.0619 | - |
| <i>D</i> ₁ | 0.1188 | - | 0.1374 | - | 0.1268 | - |
| <i>E</i> ₁ | 0.1182 | - | 0.1378 | - | 0.1279 | - |
| <i>F</i> ₁ | 0.0565 | - | 0.0741 | - | 0.0710 | - |
| <i>G</i> ₁ | 0 | -37130 | 0 | -28866 | 0 | -34703 |
| <i>H</i> ₁ | -0.0067 | - | -0.0382 | - | -0.0082 | - |
| <i>K</i> ₁ | 0 | 6800 | - | - | 0 | 4347 |

screw and the ring. The maximum flexure of the two-bearing pump at point *E* is 0.1809 mm, which is 1.326 times greater than the maximum flexure at point *D* of the three-bearing structure with a rear gear and 1.387 times greater than the maximum flexure at point *E* of the three-bearing structure with a front gear. The maximum flexure of the three-bearing structure with a front gear is only 0.006 mm less than that of the structure with a rear gear but is considerably less (by 0.0445 mm) than the flexure at the point of clutch attachment (point *A*). The flexure of the driven screw is less than that of the drive screw, but the load at the bearings is greater (Table 9). The bearing load in the three-bearing structure with a rear gear is greatest at point *G*₁ (*R*_{*G*₁} = -37130 N), where it is 1.286 times the load in the two-bearing pump and 1.07 times the load in a three-bearing structure with a front gear.

Thus, the three-bearing structure with a front gear is characterized not only by better cooling but by slightly better screw rigidity and bearing load than for the structure with a rear gear. However, the bearing load is less for the two-bearing pump.

REFERENCES

1. Kukolevskii, I.I. and Baibakov, O.V., *Vintovye nasosy s vintami spetsial'nogo profilya* (Screw Pumps with Screws of Special Profile), Moscow: Mashgiz, 1963, pp. 5–27.
2. Pyzh, O.A., Kharitonov, E.S., and Egorova, P.B., *Sudovye vintovye nasosy* (Marine Screw Pumps), Leningrad: Sudostroenie, 1969.
3. Zhenovak, N.G., *Sudovye vintovye negermetichnye nasosy* (Nonsealed Marine Screw Pumps), Leningrad: Sudostroenie, 1972.
4. Zhmud, A.E., *Vintovye nasosy s tsikloidal'nym zatsepleniem* (Screw Pumps with Cycloid Engagement), Moscow: Mashgiz, 1963.
5. Hamelberg, F.W., *Untersuchungen an Pumpen. Lauferprofile, Lauferkräfte und Leistungen von Schaubenpumpen: VDI Forschungsheft 527*, Dusseldorf: VDI Verlag, 1968, pp. 5–28.
6. Ryazantsev, V.M., Vdovenkov, V.A., and Pisarev, V.A., Determining the Forces on the Screws of a Two-Screw Pump, *Khim. Neft. Mashinostr.*, 1978, no. 3, pp. 15–17.
7. Ryazantsev, V.M., A8 2VV 50/40-30/40 Multiphase Two-Screw Pump at a Differential Pressure of 40 Bar, *Vestn. Mashinostr.*, 2006, no. 2, pp. 3–7.
8. Ryazantsev, V.M., A8 2VV 80/40-40/40 Multiphase Two-Screw Pump, *Khim. Neftegaz. Mashinostr.*, 2005, no. 4, pp. 26, 27.
9. Ryazantsev, V.M. and Plyasov, V.V., A8 2VV 125/40-80/40 Multiphase Two-Screw Pump at a Differential Pressure of 40 Bar, *Khim. Neftegaz. Mashinostr.*, 2006, no. 11, pp. 26–28.
10. Ryazantsev, V.M. and Plyasov, V.V., Moderate-Pressure Multiphase Two-Screw Pump with Small Supply, *Khim. Neftegaz. Mashinostr.*, 2008, no. 7, pp. 26, 27.
11. Ryazantsev, V.M., *Rotorno-vrashatel'nye nasosy s tsikloidal'nymi zatsepleniymami* (Rotary Pumps with Cycloid Engagement), Moscow: Mashinostroenie, 2005.